의학박사 학위논문

균일한 크기의 미세철분기반 나노입자의 T1 자기공명영상조영제로서의 특성에 관한 연구

Investigation of the characteristics of new uniform and extremely small-sized iron-based nanoparticle as a T1 contrast agent in magnetic resonance imaging

2020년 2월

서울대학교 대학원

의학과 영상의학 전공

소 영 호

Abstract

Investigation of the characteristics of new uniform and extremely small-sized iron-based nanoparticle as a T1 contrast agent in magnetic resonance imaging

Young Ho So

College of medicine, radiology

The Graduate School

Seoul National University

Background and purpose: The magnetic resonance (MR) contrast agents are generally categorized into the paramagnetic and superparamagnetic agents according to their effects on the magnetic field. Contrast-enhanced magnetic resonance angiography (MRA) is usually performed using gadolinium-based paramagnetic agents. However, owing to the potential toxicity of gadolinium free ion, it must be bound to ligands for its use as contrast agent. Half-life of gadolinium-based contrast agents (GBCAs) is about 90 minutes in patients with normal renal function, but it is prolonged from 30 to 120 hours in patients with chronic renal failure. During this time, dissociated gadolinium ion can compete with calcium ion and cause nephrogenic systemic fibrosis (NSF). Therefore, GBCAs have been considered as the causative agent in NSF. Recently, with the use

of macrocyclic GBCA, the incidence of NSF has considerably decreased. However, it was also attributed to the avoidance of GBCA in high risk patients and excessive dose administration. In contrast of GBCAs, iron oxide nanoparticles have no risk of NSF despite of its long half-life in the blood. Recently, small-sized iron nanoparticles with less than 50 nm crystalline iron oxide core were introduced in the contrast-enhanced MRA with the property of its T1 shortening effect. The purpose of this study was to evaluate the MR characteristics and the applicability of the new uniform and extremely small-sized iron oxide nanoparticles (ESIONs) with 3 – 4 nm iron core in the contrast-enhanced MRA through the phantom and animal experiments.

Methods: Using the seven ESIONs (KEG1 – 7), phantom and animal study were performed with 1.5T, 3T, and 4.7T scanners. With the phantom prepared with wide range dilutions of ESIONs, MR imaging was performed to evaluate the MR characteristics of the ESIONs using inversion-recovery turbo spin-echo (IR-TSE), multiple echo-spin echo (ME-SE), and multislice multiecho (MSME) sequences. In gradient echo sequences, MR imaging was performed with the ESIONs selected by the phantom studies (KEG1, 5) to evaluate the signal intensity of ESIONs in variable flip angles and concentrations. With the ESIONs selected by the phantom studies (KEG1, 3, 5), in vivo kinetics evaluation and in vivo cross-over studies were performed in eight rabbits using three-dimensional fast low angle shot (3D FLASH) sequence. In vivo kinetics evaluation was performed with KEG5, and the contrast enhancement over time, organ enhancement, and elimination from the

body were evaluated. The cross-over study was performed with two kinds of ESIONs (KEG1, 3) and Gd-DOTA (Dotarem®) with half-dilution (KEG1-H and KEG3-H: 0.047 mmol/kg; DOT-H: 0.05 mmol/kg) and without dilution (KEG1-S and KEG3-S: 0.093 mmol/kg; DOT-S: 0.1 mmol/kg). The between-group differences of contrast enhancement were assessed by using linear-mixed effects model. Commercially available contrast media (Dotarem®) was used in phantom and animal studies as a control group.

Results: All ESIONs were applicable for MRA with the relaxivity ratios (r_2/r_1) 6 or less than 6 at 1.5T (KEG1, 2.95; KEG2, 6.00; KEG3, 2.44; KEG4, 2.51; KEG5, 1.85; KEG6, 4.37; KEG7, 3.32) and 3T (KEG1, 3.01; KEG2, 5.72; KEG3, 2.68; KEG4, 3.40; KEG5, 3.17; KEG6, 3.76; KEG7, 4.78). The relaxivity ratio (r_2/r_1) increased with increasing magnetic field strengths. In gradient echo sequence, the peak signal intensities of the ESIONs in lowest concentration were observed in flip angles between 10° and 20° at 1.5T, and 10° and 15° at 3T, respectively. The peak signal intensities were observed in higher flip angles with an increase of concentration of ESIONs at 1.5T and 3T. In the in vivo kinetics study, KEG5 showed peak signal intensity at the first-pass images and persistent vascular enhancement until 90 minute delayed images. KEG5 showed similar organ enhancement compared to Dotarem® at all regions in the first-pass images. On the one week follow up images, KEG5 was nearly washed out from the vascular structures and the organs. In the in vivo cross-over study, all half-diluted ESIONs showed significantly lower signal intensities than their non-diluted ones at all

regions in immediate post-contrast images (KEG1-S vs. KEG1-H – difference 70.167, p<0.001 and KEG3-S vs. KEG3-H – difference 118.167, p<0.001 at aortic arch; KEG1-S vs. KEG1-H – difference 134.667, p<0.001 and KEG3-S vs. KEG3-H – difference 131.333, p<0.001 at descending thoracic aorta). In terms of peak signal intensities on the first-pass images, there was no statistical difference between KEG3-S and DOT-S (difference -8.167, p=1.000 at aortic arch; difference -3.667, p=1.000 at descending thoracic aorta), but KEG3-S and DOT-S showed significantly higher peak signal intensities than KEG1-S at all regions (p<0.05 at aortic arch and descending thoracic aorta). On the post-contrast 10 minute images, KEG3-S and KEG1-S showed significantly higher signal intensities than DOT-S at all regions (KEG3-S vs. DOT-S – difference 150.667, p<0.001 and KEG1-S vs. DOT-S – difference 71.667, p<0.001 at aortic arch; KEG3-S vs. DOT-S – difference 202.667, p<0.001 and KEG1-S vs. DOT-S – difference 127.333, p<0.001 at descending thoracic aorta).

Conclusions: On the phantom study, the ESIONs with 3 – 4 nm iron oxide cores showed good T1 shortening effect with the relaxivity ratios (r_2/r_1) 6 or less than 6 at 1.5T and 3T. On in vivo experiment, the ESION with 3 nm iron core and 10 nm overall size (KEG3) showed comparable performance on the first-pass imaging and superior performance on delayed imaging to the commercially available T1 MR contrast agent (Dotarem®) at 3T.

Keywords: iron oxide nanoparticle, blood pool contrast agent, MR angiography,

contrast enhancement

Student number: 2010-30524

Contents

List of tables

List of figures

Introduction

Since the recent introduction of 3T magnetic resonance (MR) scanners and the application of 3D gradient echo sequence, contrast-enhanced magnetic resonance angiography (CE-MRA) has become an accurate technique for the evaluation of most vascular structures (1-3). CE-MRA is usually performed using gadolinium-based blood pool agents and spatial resolution of MR images can be improved due to T1 shortening effect (4, 5). However, owing to the potential toxicity of gadolinium ion, it must be bound to ligands for its use as a contrast agent. The half-life of gadolinium-based contrast agents (GBCA) is about 90 minutes in patients with normal renal function, but it is prolonged from 30 to 120 hours in patients with chronic renal failure. During this time, dissociated gadolinium ion can compete with calcium ion and cause nephrogenic systemic fibrosis (NSF). Therefore, several reports and cases indicated that GBCAs are causative agents of NSF in patients with severe renal impairment or receiving dialysis and, according to the studies, the most of reported NSF has occurred in the patients who received older linear GBCA (6-8). Recently, with the use of macrocyclic GBCA, the incidence of NSF has considerably decreased. However, it was also attributed to the avoidance of GBCA in high risk patients and excessive dose administration (9-11).

Recently, ultrasmall superparamagnetic iron oxides (USPIOs), which have less than 50 nm crystalline iron oxide core and dextran coating, were introduced in the

CE-MRA. USPIOs increase the magnetic susceptibility of the medium and they cause a phase gradient with spin dephasing leading to decreased signal in T2-weighted imaging. USPIOs also have T1 shortening effect by the reduction in the volume magnetic anisotropy and spin disorders on the surface of the nanoparticles (12). Besides, dextran coating of USPIOs protects against endocytosis of macrophage, and permitting a long plasma half-life (13, 14). With these properties, the possibility as an alternative blood pool MR contrast agent of USPIO has been emerged. With the recent advances in synthetic methods, the size reduction of magnetic nanoparticles to 3 – 4 nm has become possible with more stability in magneto-crystalline phase and the surface state, resulting in the maximized T1 shortening effect of magnetic nanoparticles.

The purpose of this study was to evaluate the MR characteristics and the applicability of the new uniform and extremely small-sized iron oxide nanoparticles (ESIONs) with 3 – 4 nm iron core in the contrast-enhanced MRA through the phantom and animal experiments.

Materials and Methods

This study was approved by the Institutional Animal Care and Use Committee (IACUC) at Seoul National University Hospital.

Characteristics of ESIONs

Seven different kinds of ESIONs (KEG1 – 7, Hanwha Chemical Corp. Seoul, Korea) with 3 – 4 nm iron oxide nanoparticle cores were used in this study. Structurally, the ESIONs are capped with polyethylene glycol-derivatized phosphine oxide (PO-PEG), called 'surface ligand' that makes the ESIONs have high colloidal stability and biocompatibility in an aqueous medium. ESIONs were synthesized by thermal decomposition of iron-oleate complex in the presence of oleic acid and oleyl alcohol in diphenyl ether (14). After synthesis of ESIONs, ligands exchange with PO-PEG was performed to avoid aggregation and to have hydrophilic property because ESIONs were synthesized nonhydrolytically and typically coated with hydrophobic ligands. After ligands exchange, ESIONs were dispersed in the distilled water. With surface ligand, ESIONs finally have 5 – 14 nm of overall hydrodynamic diameter. The core size of ESIONs was determined by 200 kV Field-Emission Transmission Electron Microscope (FE-TEM, JEOL-2100F; JEOL Ltd., Tokyo, Japan). The hydrodynamic diameter of ESIONs was determined by dynamic light scattering (DLS, Zetasizer Nano ZS; Malvern Instrument Ltd., Malvern, England). The core size, the overall size, and the concentration of

ESIONs were listed in table 1.

MR relaxivities of ESIONs

The sample series of each ESION were prepared in 1.5ml cylindrical tubes by serial dilution with normal saline, using dilution factors of 1:1, 1:2, 1:4, 1:8, 1:16, 1:32, 1:64, and 1:128, respectively. The undiluted maximum concentrations of ESIONs were as follows: KEG1 19.73 mmol/L, KEG2 56.32 mmol/L, KEG3 66.37 mmol/L, KEG4 82.87 mmol/L, KEG5 40.36 mmol/L, KEG6 18.30 mmol/L, KEG7 12.74 mmol/L, respectively. These sample series were lined up according to the descending orders of a concentration in the plastic plate with multiple wells. To compare with the MR relaxation property of the commercially available contrast media, Dotarem® (Gd-DOTA, Guerbet, Roissy CdG, France) was used as a control and the sample series were prepared with same manner (Fig. 1). To define the relaxivities in various magnetic fields, MR imaging was performed with a 1.5T (Signa, GE Heathcare, Milwaukee, WI, USA), a 3T (Tim Trio, Siemens, Erlangen, Germany), and a 4.7T (BioSpec 47/40, Bruker, Germany) MR scanners. MR room temperature was about 22℃.

MR relaxivities (r_1, r_2) are defined as the slope of the linear regression generated from a plot of the measured relaxation rate (1/T1, 1/T2) versus the concentration of the contrast media. For the determination of MR relaxivities of the ESIONs, T1 and T2 relaxation data of each sample were obtained through various T1- and T2-weighted MR images, initially. With these data, T1 and T2 mapping were

performed and the T1 and T2 relaxation curves were estimated by curve-fitting the experimental signal intensity using the basic equation (1) or (2), and these equations were fitted monoexponentially by using Matlab (version 7.1). Based on the each relaxation curves, the relaxation times (T1 and T2) were obtained.

$$SI\ (TI) = S_0\ (1 - 2e^{-TI/T1}) \quad (1)$$

$$SI\ (TE) = S_0\ (e^{-TE/T2}) \quad (2)$$

where SI (TI) or SI (TE) indicate the signal intensity as a function of TI or TE, respectively, and S_0 corresponds to the steady-state signal intensity.

Various T1-weighted images for T1 relaxation curves were acquired with an inversion-recovery turbo spin-echo (IR-TSE) pulse sequence at several inversion times (TI) at 1.5T and 3T, and with a multislice multiecho (MS-ME) sequence at 4.7T. At 1.5T, following parameters were used: repetition time (TR) = 4400 millisecond, the echo time (TE) = 7.62 millisecond, echo train lengths (ETL) = 2, slice thickness = 2 mm, inversion times (TI) = 50, 60, 70, 80, 90, 100, 150, 200, 250, 300, 350, 400, 500, 600, 800, 1000, 1200, 1500, 2000, 2500, and 3000 millisecond, matrix for phantom measurement = 256 x 256. At 3T, following parameters were used: TR = 4000 millisecond, TE = 14 millisecond, ETL = 2, slice thickness = 5 mm, TI = 25, 50, 75, 100, 150, 200, 250, 300, 350, 400, 500, 600, 800, 1000, 1500, 2000, 2500, 3000, and 3500 millisecond, matrix for phantom measurement = 228 x 384. At 4.7T, following parameters were used: TR = 70 - 8000 millisecond (8 point), TE = 7.76 millisecond, ETL = 1, slice thickness = 1 mm, matrix for phantom measurement = 128 x 128.

Various T2-weighted images for T2 relaxation curves were acquired with a multiple echo-spin echo (ME-SE) pulse sequence with multiple echo times at 1.5T and 3T, and with a MS-ME sequence at 4.7T. At 1.5T, following parameters were used: TR = 5000 millisecond, TE = 15, 20, 25, 30, 35, 40, 45, 50, 55, 60, 70, 75, 80, 100, 110, 105, 140, 165, and 220 millisecond, ETL = 1, slice thickness = 1 mm, matrix for phantom measurement = 256 x 256. At 3T, following parameters were used: TR = 5000 millisecond, TE = 16, 20, 32, 40, 48, 50, 60, 64, 80, 100, 150, and 200 millisecond, ETL = 1, slice thickness = 2 mm, matrix for phantom measurement = 160 x 256. At 4.7T, following parameters were used: TR = 10000 millisecond, TE = 7.5 - 1920 millisecond (256 point), ETL = 1, slice thickness = 1 mm, matrix for phantom measurement = 128 x 128.

After obtainment of relaxation times, r_1 and r_2 were calculated by linear fitting with use of the equation (3).

$$\frac{1}{\text{Ti (measured)}} = \frac{1}{\text{Ti (solution)}} + r_i \cdot [\text{concentration of contrast material}] \qquad (3)$$

where Ti (measured) indicates the longitudinal (T1) or transverse (T2) relaxation times of a solution containing contrast material and Ti (solution) indicates the relaxation times of the solvent without contrast material.

The mean signal intensities of the samples were measured by using a measurement tool equipped in PACS system (Maroview 5.4, Infinitt, Seoul, Korea). The mean signal intensities were measured under the assumption that the background signal was constant. The region of interest (ROI) of each sample was located in the middle of the image slice having largest diameter.

In vitro MR imaging of ESIONs in gradient echo sequences

In the gradient echo sequences, MR imaging was performed with two selected ESIONs showing good T1 shortening effect (KEG1, KEG5) to evaluate the signal intensity with variable flip angles and concentrations. Each ESION and Dotarem® was prepared in 5 ml cylindrical tubes by variable dilution with normal saline. The undiluted maximum concentration of ESIONs and Dotarem® were as follows: KEG1 17.94 mmol/L, KEG5 13.45 mmol/L, and Dotarem® 19.08 mmol/L, respectively. The serially diluted samples were listed in table 2. MRA imaging sequence was performed with fast spoiled gradient recalled (FSPGR) at 1.5T and fast low angle shot (FLASH) at 3T MR scanners. In FSPGR sequence, following parameters were used: TR = 5.26 millisecond, TE = 1.89 millisecond, FA = 5°, 10°, 15°, 20°, 25°, 30°, 35°, 40°, 45°, 50°, 60°, slice thickness = 5 mm, NEX = 1, matrix = 256 x 192. In FLASH sequence, following parameters were used: TR = 4.05 millisecond, TE = 1.54 millisecond, FA = 5°, 10°, 15°, 20°, 25°, 30°, 35°, 40°, 50°, 60°, 70°, 80°, 90°, slice thickness = 5 mm, NEX = 1, matrix = 269 x 448.

The signal intensities of the samples were measured by using a measurement tool equipped in PACS system (Maroview 5.4, Infinitt, Seoul, Korea). The changes of contrast enhancement were evaluated with the various flip angles in each concentration. The signal intensities were measured under the assumption that the background signal was constant.

In vivo kinetics of ESIONs

To evaluate in vivo kinetics of ESIONs, MRA was performed with a selected ESION showing good T1 shortening effect (KEG5). To compare with the commercially available MR contrast media, Dotarem® was used as a control.

Two forty-week-old New Zealand White rabbits (weight: 3kg) were prepared for MRA. Complete anesthesia was achieved after intramuscular injection of ketamine hydrochloride (ketamine 100mg/kg IM). The marginal ear vein was catheterized for delivery of contrast materials using 24-gauge peripheral intravenous angiocatheter. Animal was placed supine position in a standard head coil and the abdomen centered in the magnet (3T, Tim Trio, Siemens). The doses of KEG5 and Dotarem® were 0.093 mmol/kg and 0.1 mmol/kg, respectively. After pre-contrast images were obtained, contrast material was infused as a bolus with a constant rate during 10 seconds with hands. MRA was performed under care bolus technique at left ventricle after contrast material administration. The sequence used for MRA was 3D FLASH and the following parameters were used: TR = 2.8 millisecond, TE = 1.0 millisecond, FA = 20°, TE = 1.0 millisecond, slice thickness = 1 mm, NEX = 1, FOV = 140x280.

The vascular enhancement over time, the organ enhancement, and the clearance of the ESION were evaluated. MR images were obtained at pre- and immediate post-contrast injection, post-contrast 3, 5, 10, 20, 40, 60, 90 minute, and one week later. The mean signal intensities of immediate post-contrast image were measured at left ventricle, aortic arch, carotid artery, descending thoracic aorta, ascending aorta,

right iliac artery, left iliac artery, right kidney cortex and medulla, liver, psoas muscle, and bladder. The mean signal intensities of post 3, 5, 10, 20, 40, 60, and 90 minute were measured at left ventricle and descending thoracic aorta. The mean signal intensities of target regions were measured by using a measurement tool equipped in PACS system (Maroview 5.4, Infinitt, Seoul, Korea). The signal intensities were measured under the assumption that the background signal was constant.

In vivo cross-over experiment

To evaluate the diagnostic performance of the ESIONs in CE-MRA, cross-over experiment using two 3 nm-sized ESIONs with different surface ligands (KEG1, KEG3) and Dotarem® was performed in rabbits. Contrast agents were prepared with a clinical dose and a half-diluted clinical dose: 0.093 mmol/kg KEG1 and KEG3 (KEG1-S and KEG3-S), 0.047 mmol/kg KEG1 and KEG3 (KEG1-H and KEG3-H), and 0.1 mmol/kg Dotarem® (DOT-S) and 0.05 mmol/kg Dotarem® (DOT-H).

MRA was performed in six 40-week-old New Zealand White rabbits (weight: 3kg). Animal preparation and MRA protocols were same as previous in vivo study. MRA was performed with cross-over design, i.e., three contrast materials with two different doses were applied each rabbit by turns in 6 rabbits.

MR images were obtained at pre- and immediate post-contrast injection, post-contrast 1, 5, and 10 minute. The mean signal intensities were measured at aortic

arch and descending thoracic aorta. The mean signal intensities of target regions were measured by using a measurement tool equipped in PACS system (Maroview 5.4, Infinitt, Seoul, Korea). The signal intensities were measured under the assumption that the background signal was constant. The differences of contrast enhancement between six contrast agents were evaluated.

Statistical analysis for cross-over experiment was performed to assess between-group differences by using linear-mixed effects model. Differences with adjusted p-values less than 0.05 were considered significant (accounting for a Bonferroni correction). Statistical analysis was performed with R version 3.4.5 (http://r-project.org).

Results

MR relaxivities of ESIONs

For the determination of MR relaxivities of the ESIONs, multiple T1- and T2-weighted MR images were obtained with IR-TSE and ME-SE sequences (Fig. 2). Relaxation curves (Fig. 3) were obtained based on various T1- and T2- weighted images. T1 and T2 values of serially diluted samples obtained from the relaxation curves were listed in table 3 and 4. MR relaxivities (r_1, r_2) were calculated by the linear regression generated from a plot of the measured relaxation rate (1/T1, 1/T2) versus the concentration of the contrast media (Fig. 4). The calculated relaxivity (r_1, r_2) and relaxivity ratio (r_2/r_1) at 1.5T, 3T, and 4.7T were listed in table 5. The highest relaxivities r_1 of the ESIONs were found at 1.5T (KEG1, 5.79 $mM^{-1}s^{-1}$; KEG2, 2.95 $mM^{-1}s^{-1}$; KEG3, 7.60 $mM^{-1}s^{-1}$; KEG4, 4.86 $mM^{-1}s^{-1}$; KEG5, 8.40 $mM^{-1}s^{-1}$; KEG6: 6.73 $mM^{-1}s^{-1}$; KEG7, 6.20 $mM^{-1}s^{-1}$). The relaxivity r_1 decreased with increasing magnetic field strengths. Relaxivity r_2 of ESIONs showed no significant changes from 1.5T to 3T, but increased at 4.7T. The lowest relaxivity ratios (r_2/r_1) of ESIONs were found at 1.5T (KEG1, 2.95; KEG2, 6.00; KEG3, 2.44; KEG4, 2.51; KEG5, 1.85; KEG6, 4.37; KEG7, 3.32). The relaxivity ratios increased with increasing magnetic field strengths. In case of Dotarem®, the change of relaxivity r_1 and relaxivity ratio (r_2/r_1) showed similar pattern compare to the ESIONs. At 1.5T and 3T, all ESIONs showed relaxivity ratio (r_2/r_1) 6 or less than 6, which were satisfactory values for showing good T1 shortening effect (KEG1, 2.95 at 1.5T and

3.01 at 3T; KEG2, 6.00 at 1.5T and 5.72 at 3T; KEG3, 2.44 at 1.5T and 2.68 at 3T; KEG4, 2.51 at 1.5T and 3.40 at 3T; KEG5, 1.85 at 1.5T and 3.17 at 3T; KEG6, 4.37 at 1.5T and 3.76 at 3T, KEG7, 3.32 at 1.5T and 4.78 at 3T) (Fig. 5).

In vitro MR imaging of ESIONs in gradient echo sequences

The signal intensities of ESIONs and Dotarem® in relation to the variable flip angles were illustrated in figure 6. At 1.5T, the peak signal intensities of KEG1 and KEG5 with the lowest concentration (1.79 mmol/L and 0.54 mmol/L) were observed in 20° and 10° of flip angles, respectively, and the peak signal intensities of the ESIONs were observed in higher flip angle with the increase of the concentration until 50° of flip angle. At 3T, the peak signal intensities of KEG1 and KEG5 with the lowest concentration (1.79 mmol/L and 0.54 mmol/L) were observed in 15° and 10° of flip angles, respectively, and the peak signal intensities of the ESIONs were observed in higher flip angle with the increase of the concentration until 50° and 40°, respectively. In case of the same concentration of ESIONs, the peak signal intensities were observed in lower flip angles at 3T than at 1.5T. The ranges of the flip angles showing peak signal intensity of ESIONs were between 10° and 50° at both 1.5T and 3T. The changes of peak signal intensity of Dotarem® showed similar patterns compare to the ESIONs at 1.5T and 3T.

In vivo kinetics of ESIONs

On the subjective image quality evaluation of the immediate post-contrast images, KEG5 showed excellent contrast of the vascular lumen with main aortic branches being well visualized such that the entire course and luminal status can be fully evaluated with confidence. When the vascular enhancement patterns over time were evaluated, KEG5 showed persistent vascular enhancement from the immediate post-contrast phase to the 90 minute delayed phase. Dotarem® showed vascular enhancement just on the immediate post-contrast phase and nearly washed out from the vascular structures on the five minute images (Fig. 7). The mean signal intensity changes over time at aortic arch and descending thoracic aorta were illustrated in figure 8.

In terms of organ enhancement, KEG5 showed similar enhancement compare to Dotarem® at all regions in the immediate post-contrast images (Fig. 9).

On the one week follow up images, KEG5 was nearly washed out from the vascular structures and the organs (Fig. 7).

In vivo cross-over experiment

The MR images and the signal intensities obtained from in vivo cross-over experiment at aortic arch and descending thoracic aorta are shown in figure 10 and table 6. The signal intensity changes over time were illustrated in figure 11.

All ESIONs and Dotarem® showed peak signal intensity on the immediate post-contrast images. The signal intensities of Dotarem® showed abrupt decrease on the post-contrast 1 minute images, whereas the signal intensities of all ESIONs showed

slight decrease on the post-contrast 1 minute images. The signal intensities of all ESIONs were reached a plateau at post-contrast 1 minute, and the plateau was maintained until post 10 minute.

All half-diluted contrast materials showed significantly lower signal intensities than their non-diluted ones at all regions in immediate post-contrast images (DOT-S vs. DOT-H – difference 107.833, $p<0.001$ and KEG1-S vs. KEG1-H – difference 70.167, $p<0.001$ and KEG3-S vs. KEG3-H – difference 118.167, $p<0.001$ at aortic arch; DOT-S vs. DOT-H – difference 141.833, $p<0.001$ and KEG1-S vs. KEG1-H – difference 134.667, $p<0.001$ and KEG3-S vs. KEG3-H – difference 131.333, $p<0.001$ at descending thoracic aorta). On the post-contrast 10 minute images, half-diluted ESIONs showed significantly lower signal intensities than their non-diluted ones (KEG1-S vs. KEG1-H – difference 57.000, $p=0.008$ and KEG3-S vs. KEG3-H – difference 106.667, $p<0.001$ at aortic arch; KEG1-S vs. KEG1-H – difference 99.000, $p<0.001$ and KEG3-S vs. KEG3-H – difference 133.000, $p<0.001$ at descending thoracic aorta), but there was no statistical difference of the signal intensities between half-diluted Gd-DOTA and non-diluted Gd-DOTA (DOT-S vs. DOT-H – difference 3.833, $p=1.000$ at aortic arch; difference -0.833, $p=1.000$ at descending thoracic aorta).

In terms of peak signal intensities on the immediate post-contrast images, there was no statistical difference between KEG3-S and DOT-S (difference -8.167, $p=1.000$ at aortic arch; difference -3.667, $p=1.000$ at descending thoracic aorta), but KEG3-S and DOT-S showed significantly higher peak signal intensities than

KEG1-S in all regions (KEG3-S vs. KEG1-S – difference 85.500, $p<0.001$ and KEG1-S vs. DOT-S – difference -93.667, $p<0.001$ at aortic arch; KEG3-S vs. KEG1-S – difference 71.167, $p=0.011$ and KEG1-S vs. DOT-S – difference -74.833, $p=0.006$ at descending thoracic aorta). On the post-contrast 10 minute images, KEG3-S and KEG1-S showed significantly higher signal intensities than DOT-S at all regions (KEG3-S vs DOT-S – difference 150.667, $p<0.001$ and KEG1-S vs. DOT-S – difference 71.667, $p<0.001$ at aortic arch; KEG3-S vs DOT-S – difference 202.667, $p<0.001$ and KEG1-S vs. DOT-S – difference 127.333, $p<0.001$ at descending thoracic aorta) (Table 7, 8).

Table 1. The iron core size, overall size, and maximum concentration of ESIONs.

	core size (nm)	overall size (mean) (nm)	maximum concentration (mmol/L)
KEG1	3	5	19.73
KEG2	4	6	56.32
KEG3	3	10	66.37
KEG4	4	12	82.87
KEG5	3	13	40.36
KEG6	3	5	18.30
KEG7	3	14	12.74
Gd-DOTA	NA	NA	133.55

ESIONs – extremely small-sized iron oxide nanoparticles

NA – not avaliable

Table 2. The concentrations of ESIONs used in in vitro MR imaging with gradient echo sequences.

	KEG1 (mmol/L)	KEG5 (mmol/L)	Dotarem (mmol/L)
Concentration	17.94	13.45	19.08
	14.35	10.76	15.26
	10.76	8.07	11.45
	7.17	5.38	7.63
	5.38	2.69	3.82
	3.59	1.08	1.53
	1.79	0.81	1.14
		0.54	0.76

ESIONs – extremely small-sized iron oxide nanoparticles

MR – magnetic resonance

Table 3. T1 and T2 values of a series of diluted ESIONs at 1.5T.

	Dilution	Contrast materials							
	factor	KEG1	KEG2	KEG3	KEG4	KEG5	KEG6	KEG7	Dotarem
	1:1	NA	NA	NA	NA	NA	NA	NA	NA
	1:2	17.97	NA	NA	NA	NA	18.15	26.15	NA
	1:4	33.99	24.64	NA	NA	NA	31.98	50.10	NA
T1	1:8	67.00	47.49	NA	19.50	23.13	58.98	87.65	NA
[ms]	1:16	114.59	90.22	30.75	38.61	44.52	115.35	177.13	NA
	1:32	216.56	178.75	58.51	71.82	82.91	221.07	322.42	30.08
	1:64	403.11	342.43	105.68	135.16	153.64	402.59	574.47	58.05
	1:128	717.37	585.85	218.36	260.57	302.88	511.44	947.82	111.8
	1:1	NA	NA	NA	NA	NA	NA	NA	NA
	1:2	13.26	NA	NA	NA	NA	NA	17.16	NA
	1:4	16.08	18.99	NA	NA	NA	18.72	29.76	NA
T2	1:8	46.59	20.03	15.62	NA	NA	31.02	54.65	17.00
[ms]	1:16	83.43	32.50	24.03	19.60	23.55	64.99	102.22	26.97
	1:32	156.18	63.66	51.04	29.59	39.93	141.62	192.07	52.36
	1:64	373.00	136.90	73.82	55.03	69.29	NA	342.21	100.64
	1:128	NA	NA	NA	98.61	133.47	NA	NA	NA

ESIONs – extremely small-sized iron oxide nanoparticles

ms – millisecond

NA – not available

Table 4. T1 and T2 values of a series of diluted ESIONs at 3T.

	Dilution	Contrast materials							
	factor	KEG1	KEG2	KEG3	KEG4	KEG5	KEG6	KEG7	Dotarem
	1:1	NA	NA	NA	NA	NA	NA	NA	NA
	1:2	22.94	NA	NA	NA	NA	NA	37.89	NA
	1:4	37.46	NA	NA	NA	NA	37.33	68.70	NA
T1	1:8	82.65	59.14	21.52	27.05	31.16	82.94	141.0	7.99
[ms]	1:16	154.7	119.9	37.45	52.38	60.43	161.0	266.0	17.06
	1:32	293.7	240.0	79.65	101.7	115.0	302.5	483.2	32.48
	1:64	528.2	453.4	151.3	192.7	205.1	539.1	799.9	61.61
	1:128	897.4	750.0	289.3	357.2	390.9	892.1	1095	116.9
	1:1	NA	NA	NA	NA	NA	NA	NA	NA
	1:2	9.76	NA	NA	NA	NA	NA	16.77	NA
	1:4	14.17	NA	NA	NA	NA	11.89	17.02	NA
T2	1:8	25.47	13.38	9.54	10.47	11.68	20.26	29.29	7.197
[ms]	1:16	50.34	20.81	13.52	15.64	20.26	39.99	58.00	13.73
	1:32	99.56	40.49	24.32	27.84	39.62	82.71	109.75	27.55
	1:64	200.33	81.60	45.92	54.84	71.93	169.36	211.91	56.16
	1:128	401.45	160.36	88.20	104.91	142.66	301.66	406.11	110.20

ESIONs – extremely small-sized iron oxide nanoparticles

ms - millisecond

NA – not available

Table 5. Relaxivities and relaxivity ratios of ESIONs and Dotarem.

	1.5T			3T			4.7T		
	r_1^*	r_2^*	r_2/r_1	r_1^*	r_2^*	r_2/r_1	r_1^*	r_2^*	r_2/r_1
KEG1	5.79	17.10	2.95	5.30	15.93	3.01	3.66	20.17	5.51
KEG2	2.95	17.72	6.00	2.38	13.61	5.72	1.41	18.03	12.79
KEG3	7.60	18.54	2.44	6.41	17.17	2.68	3.65	23.89	6.55
KEG4	4.86	12.19	2.51	3.52	11.98	3.40	2.29	16.67	7.28
KEG5	8.40	15.57	1.85	6.01	19.07	3.17	4.42	22.77	5.15
KEG6	6.73	29.43	4.37	5.77	21.68	3.76	3.64	29.99	8.24
KEG7	6.20	20.55	3.32	4.44	21.18	4.78	3.20	30.39	9.50
Gd-DOTA	7.74	8.64	1.12	7.07	8.71	1.23	2.75	3.46	1.26

* Values in $mM^{-1}s^{-1}$ and obtained at 22°C

ESIONs – extremely small-sized iron oxide nanoparticles

Table 6. The signal intensities obtained from in vivo cross-over experiment at aortic arch and descending thoracic aorta.

		pre	immediate	Post 1 minute	Post 5 minute	Post 10 minute
Aortic arch	DOT-H	59.2.5±13.6	179.8±63.4	73.2±4.8	65.8±8.52	62.3±9.71
	DOT-S	31.2±6.5	346±56.7	107±9.6	78.2±4.9	65.7±7.3
	KEG1-H	29.7±15.2	141±36.5	104±21.1	95±19.6	88.5±19.2
	KEG1-S	34.5±9.8	258±24.7	193±24.1	173±23.5	155±24.8
	KEG3-H	28.7±11.4	212±35.7	147±27.0	137±23.1	136±25.1
	KEG3-S	32.8±8.0	340±68.8	251±39.1	256±38.0	249±34.5
Descending thoracic aorta	DOT-H	85.5±3.3	245±69.4	105±9.1	97.2±6.1	91.3±5.4
	DOT-S	66.5±21.5	387±54.6	128±16.5	95.5±8.2	90.5±7.8
	KEG1-H	71±17.6	177±26.6	141±33.1	125±30.4	119±30.7
	KEG1-S	65.7±19.5	336±42.2	252±50.3	229±47.0	218±45.6
	KEG3-H	74.8±12.5	252±46.6	180±16.2	167±22.2	160±21.7
	KEG3-S	65±17.4	405±56.1	332±40.2	310±34.4	302±41.9

DOT-H – 0.05 mmol/kg Gd-DOTA, DOT-S – 0.1 mmol/kg Gd-DOTA, KEG1-H – 0.047 mmol/kg KEG1, KEG1-S – 0.093 mmol/kg KEG1, KEG3-H – 0.047 mmol/kg KEG3, KEG3-S – 0.093 mmol/kg KEG3

Table 7. Between-group differences of the signal intensities on the immediate post-contrast images in cross-over experiment.

Region	F-statistic	p-value	Comparison	Estimate (difference)	F-statistic	p-value	adjusted p-value
Aortic arch	33.493	<0.001	DOT-S vs. DOT-H	107.833	45.012	<0.001	<0.001
			KEG1-H vs. DOT-H	-56.000	12.139	0.001	0.010
			KEG1-S vs. DOT-H	14.167	0.777	0.380	1.000
			KEG3-H vs. DOT-H	-18.500	1.325	0.252	1.000
			KEG3-S vs. DOT-H	99.667	38.452	<0.001	<0.001
			KEG1-H vs. DOT-S	-163.833	103.902	<0.001	<0.001
			KEG1-S vs. DOT-S	-93.667	33.962	<0.001	<0.001
			KEG3-H vs. DOT-S	-126.333	61.781	<0.001	<0.001
			KEG3-S vs. DOT-S	-8.167	0.258	0.612	1.000
			KEG1-S vs. KEG1-H	70.167	19.058	<0.001	<0.001
			KEG3-H vs. KEG1-H	37.500	5.444	0.021	0.315
			KEG3-S vs. KEG1-H	155.667	93.802	<0.001	<0.001
			KEG3-H vs. KEG1-S	-32.667	4.131	0.044	0.659
			KEG3-S vs. KEG1-S	85.500	28.298	<0.001	<0.001
			KEG3-S vs. KEG3-H	118.167	54.052	<0.001	<0.001
Descending thoracic aorta	32.737	<0.001	DOT-S vs. DOT-H	141.833	47.484	<0.001	<0.001
			KEG1-H vs. DOT-H	-67.667	10.808	0.001	0.019
			KEG1-S vs. DOT-H	67.000	10.596	0.001	0.021
			KEG3-H vs. DOT-H	6.833	0.110	0.740	1.000
			KEG3-S vs. DOT-H	138.167	45.061	<0.001	<0.001
			KEG1-H vs. DOT-S	-209.500	103.600	<0.001	<0.001
			KEG1-S vs. DOT-S	-74.833	13.218	<0.001	0.006
			KEG3-H vs. DOT-S	-135.000	43.019	<0.001	<0.001
			KEG3-S vs. DOT-S	-3.667	0.032	0.859	1.000
			KEG1-S vs. KEG1-H	134.667	42.807	<0.001	<0.001
			KEG3-H vs. KEG1-H	74.500	13.101	<0.001	0.006
			KEG3-S vs. KEG1-H	205.833	100.005	<0.001	<0.001
			KEG3-H vs. KEG1-S	-60.167	8.545	0.004	0.060
			KEG3-S vs. KEG1-S	71.167	11.955	0.001	0.011
			KEG3-S vs. KEG3-H	131.333	40.714	<0.001	<0.001

DOT-H – 0.05 mmol/kg Gd-DOTA, DOT-S – 0.1 mmol/kg Gd-DOTA, KEG1-H – 0.047 mmol/kg KEG1, KEG1-S – 0.093 mmol/kg KEG1, KEG3-H – 0.047 mmol/kg KEG3, KEG3-S – 0.093 mmol/kg KEG3

Table 8. Between-group differences of the signal intensities on the post-contrast 10 minute images in cross-over experiment.

Region	F-statistic	p-value	Comparison	Estimate (difference)	F-statistic	p-value	adjusted p-value
Aortic arch	26.63	<0.001	DOT-S vs. DOT-H	3.833	0.057	0.812	1.000
			KEG1-H vs. DOT-H	18.500	1.325	0.252	1.000
			KEG1-S vs. DOT-H	75.500	22.066	<0.001	<0.001
			KEG3-H vs. DOT-H	47.833	8.857	0.003	0.051
			KEG3-S vs. DOT-H	154.500	92.401	<0.001	<0.001
			KEG1-H vs. DOT-S	14.667	0.833	0.363	1.000
			KEG1-S vs. DOT-S	71.667	19.882	<0.001	<0.001
			KEG3-H vs. DOT-S	44.000	7.494	0.007	0.104
			KEG3-S vs. DOT-S	150.667	87.873	<0.001	<0.001
			KEG1-S vs. KEG1-H	57.000	12.577	0.001	0.008
			KEG3-H vs. KEG1-H	29.333	3.331	0.070	1.000
			KEG3-S vs. KEG1-H	136.000	71.598	<0.001	<0.001
			KEG3-H vs. KEG1-S	-27.667	2.963	0.087	1.000
			KEG3-S vs. KEG1-S	79.000	24.159	<0.001	<0.001
			KEG3-S vs. KEG3-H	106.667	44.043	<0.001	<0.001
Descending thoracic aorta	30.492	<0.001	DOT-S vs. DOT-H	-0.833	0.002	0.968	1.000
			KEG1-H vs. DOT-H	27.500	1.785	0.184	1.000
			KEG1-S vs. DOT-H	126.500	37.772	<0.001	<0.001
			KEG3-H vs. DOT-H	68.833	11.184	0.001	0.016
			KEG3-S vs. DOT-H	201.833	96.156	<0.001	<0.001
			KEG1-H vs. DOT-S	28.333	1.895	0.171	1.000
			KEG1-S vs. DOT-S	127.333	38.271	<0.001	<0.001
			KEG3-H vs. DOT-S	69.667	11.456	0.001	0.014
			KEG3-S vs. DOT-S	202.667	96.952	<0.001	<0.001
			KEG1-S vs. KEG1-H	99.000	23.135	<0.001	<0.001
			KEG3-H vs. KEG1-H	41.333	4.033	0.046	0.697
			KEG3-S vs. KEG1-H	174.333	71.738	<0.001	<0.001
			KEG3-H vs. KEG1-S	-57.667	7.849	0.006	0.087
			KEG3-S vs. KEG1-S	75.333	13.396	<0.001	0.005
			KEG3-S vs. KEG3-H	133.000	41.754	<0.001	<0.001

DOT-H – 0.05 mmol/kg Gd-DOTA, DOT-S – 0.1 mmol/kg Gd-DOTA, KEG1-H – 0.047 mmol/kg KEG1, KEG1-S – 0.093 mmol/kg KEG1, KEG3-H – 0.047 mmol/kg KEG3, KEG3-S – 0.093 mmol/kg KEG3

Fig. 1. A series of diluted ESIONs and Dotarem lined up according to the descending orders of a concentration in 1.5ml cylindrical tubes.

The dilution factors were 1:1, 1:2, 1:4, 1:8, 1:16, 1:32, 1:64, and 1:128, respectively. The undiluted maximum concentrations of ESIONs and Dotarem were as follows: KEG1 19.73 mmol/L, KEG2 56.32 mmol/L, KEG3 66.37 mmol/L, KEG4 82.87 mmol/L, KEG5 40.36 mmol/L, KEG6 18.30 mmol/L, KEG7 12.74 mmol/L, and Dotarem 133.55 mmol/L, respectively.

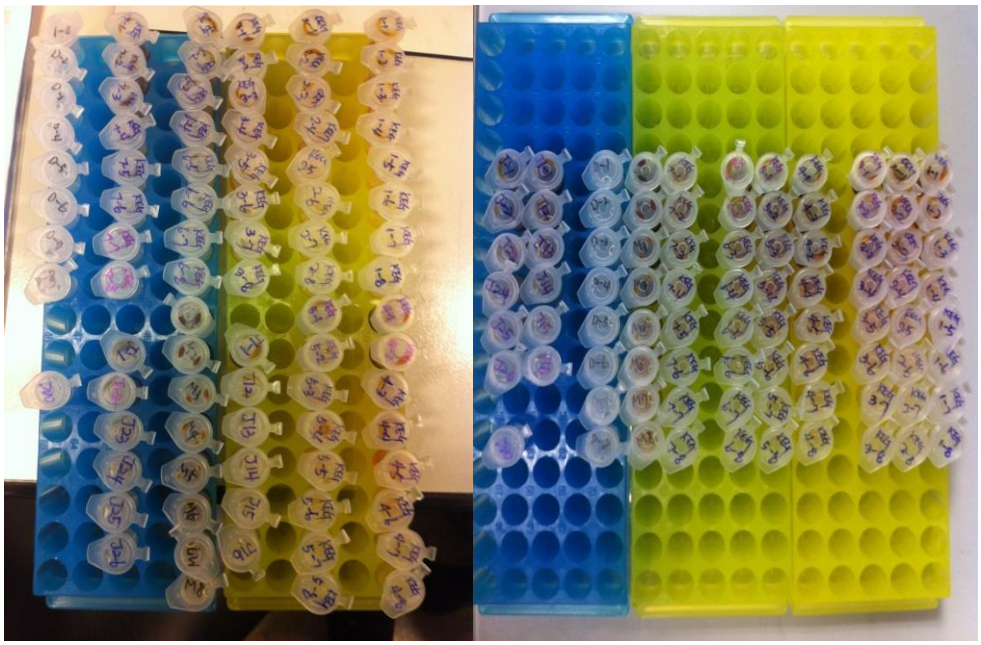

1.5T 3T

Fig. 2. The sample images of the T1 and T2-weighted images of the phantom at 1.5T and 3T scanners.

IR-TSE sequence was used for the T1-weighted images and parameters were as follows; TR = 4400 millisecond, TE = 7.62 millisecond, ETL = 2, slice thickness = 2 mm, TI = 600 millisecond, matrix = 256 x 256 at 1.5T, and TR = 4000 millisecond, TE = 14 millisecond, ETL = 2, slice thickness = 5 mm, TI = 100 millisecond, matrix for phantom measurement = 228 x 384 at 3T, respectively. ME-SE sequence was used for the T2-weighted images and the parameters were as follows; TR = 5000 millisecond, TE = 20 millisecond, ETL = 1, slice thickness = 1 mm, matrix = 256 x 256 at 1.5T, and TR = 5000 millisecond, TE = 32 millisecond, ETL = 1, slice thickness = 2 mm, matrix = 160 x 256 at 3T, respectively.

T1 weighted image at 1.5T (TI = 600 millisecond)

T2 weighted image at 1.5T (TE = 20 millisecond)

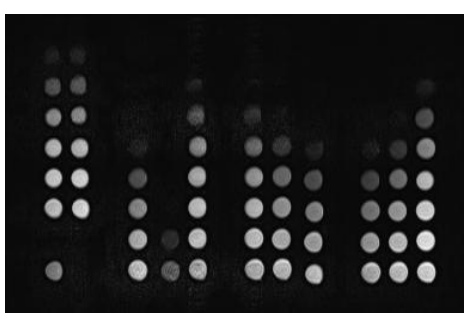

T1 weighted image at 3T (TI = 100 millisecond)

T2 weighted image at 3T (TE =32 millisecond)

Fig. 3. Relaxation curves of ESIONs (KEG1, 3, 5) and Dotarem obtained at 1.5T and 3T (dilution ratio = 1:32).

T1 and T2 relaxation curves were estimated by curve-fitting the experimental signal intensity as a function of TI and TE, respectively (equation (1) and (2) in text), and these equations were fitted monoexponentially by using Matlab (version 7.1). Based on the each relaxation curves, the relaxation times (T1 and T2) were obtained. The data were obtained at 22°C (MR room temperature).

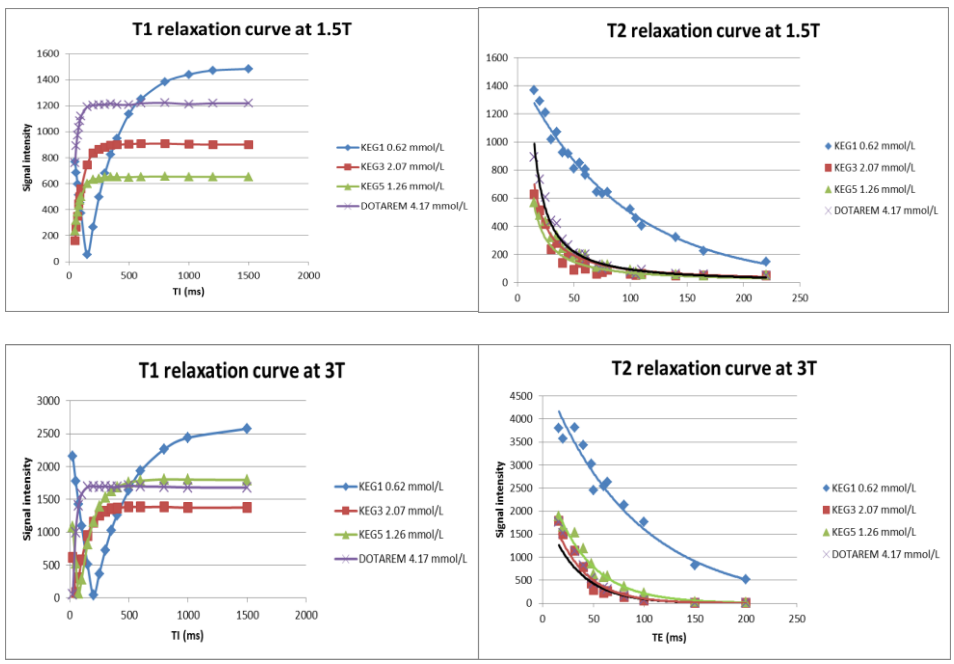

Fig. 4. The examples of the calculation of r_1 relaxivity of KEG1, 3, 5, and Dotarem at 1.5T and 3T.

MR Relaxivity (r_1) is defined as the slope of the linear regression generated from a plot of the measured relaxation rates Δ(1/T1) versus the concentration of contrast media.

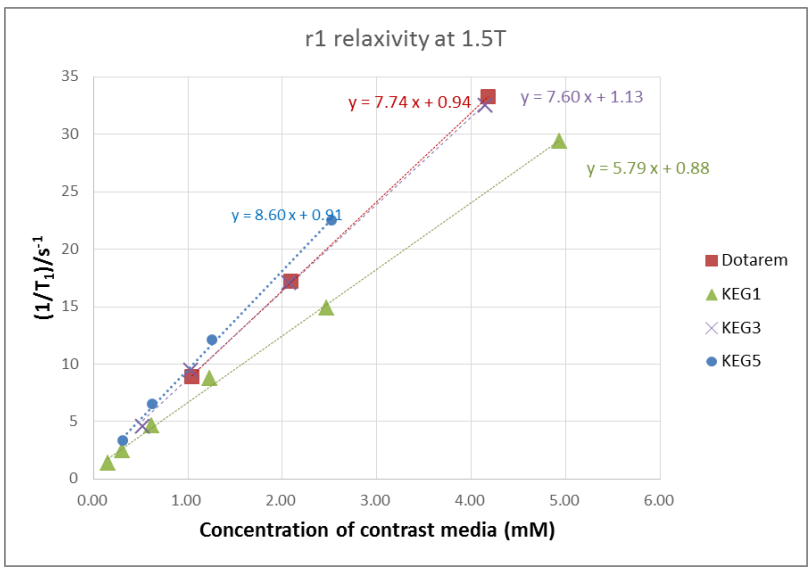

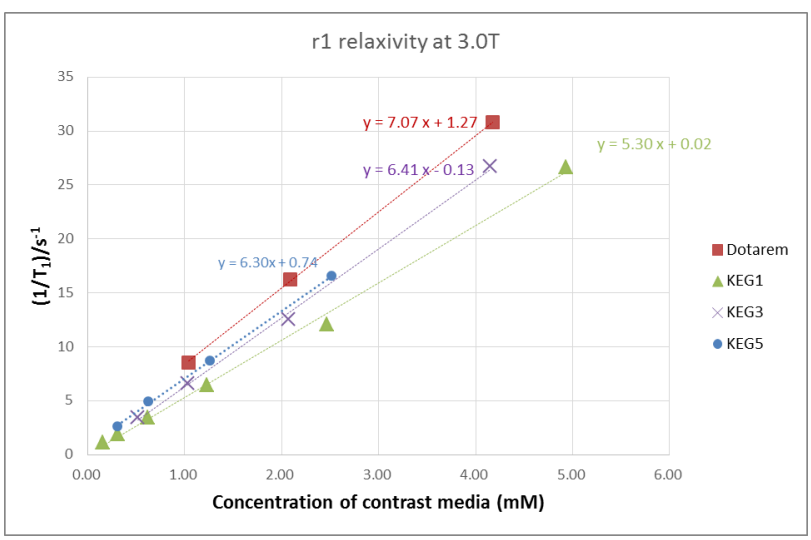

Fig. 5. Comparison of relaxivity ratios (r_2/r_1) of ESIONs and Dotarem.

Relaxivity ratio (r_2/r_1) of ESIONs increased with increasing magnetic field strengths. At 1.5T and 3T, relaxivity ratios (r_2/r_1) of ESIONs were 6 or less than 6, which were required value for showing good T1 shortening effect.

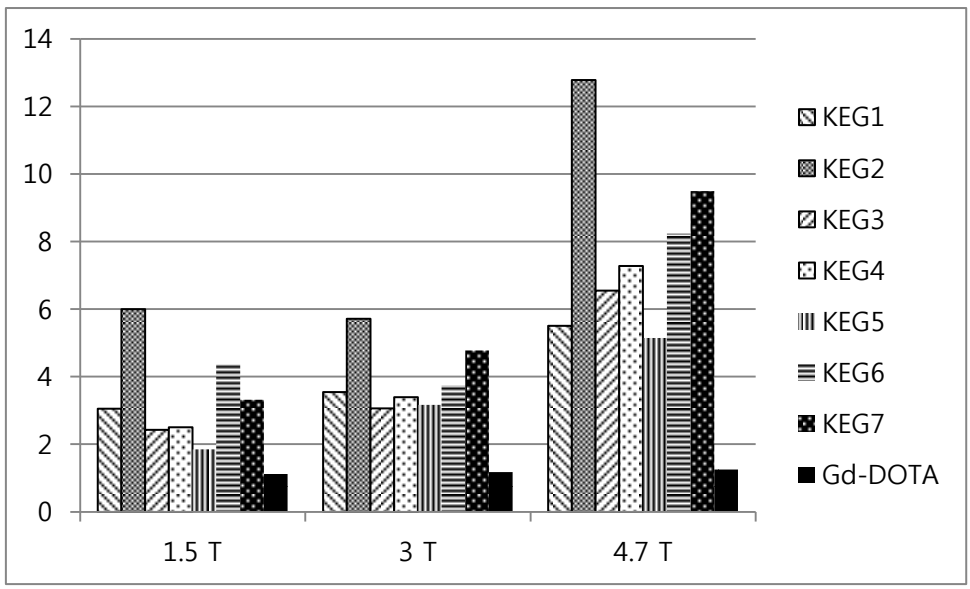

Fig. 6. The signal intensities of ESIONs and Dotarem in relation to the variable flip angles. The peak signal intensities were observed in higher flip angles with the increase of concentration. The changes of peak signal intensity of Dotarem showed similar patterns compare to the ESIONs.

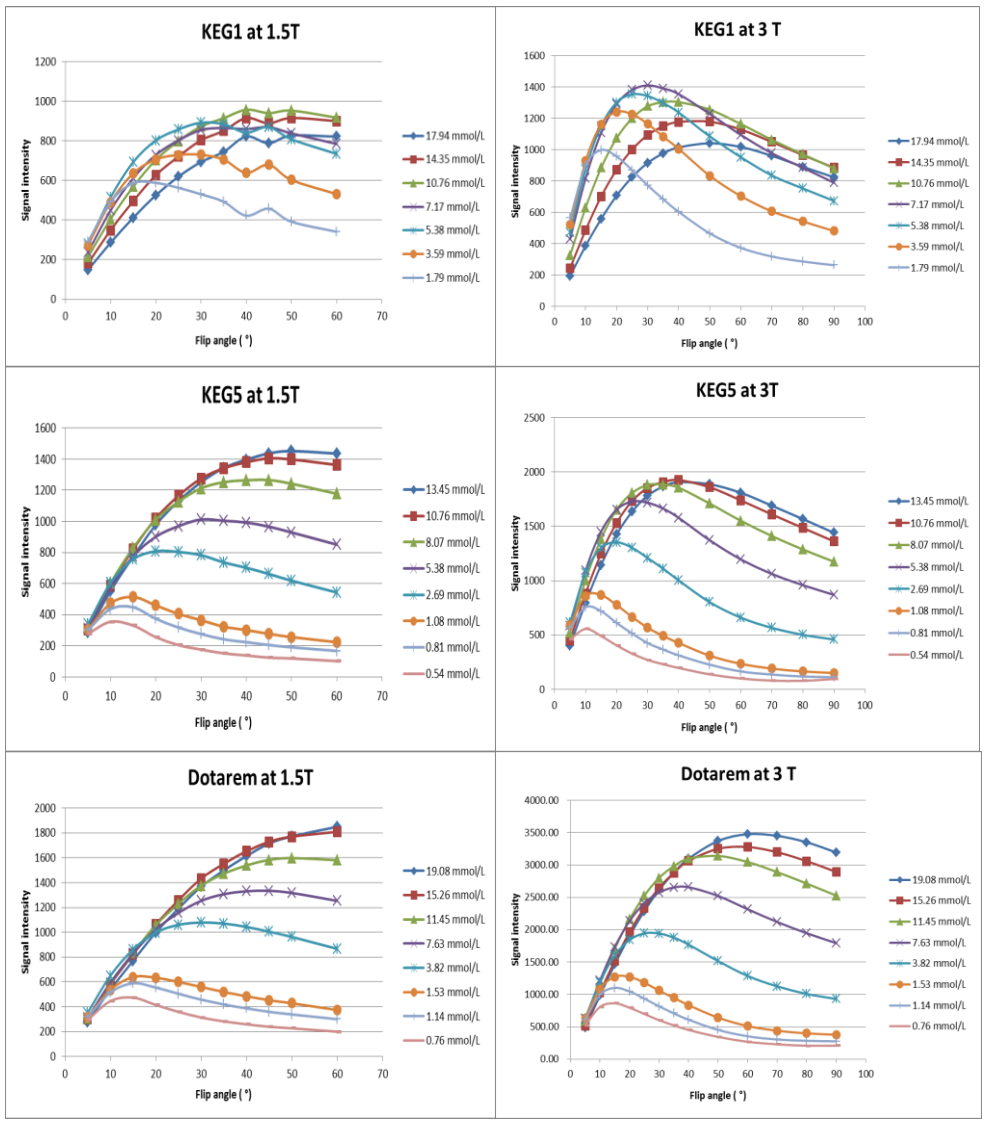

Fig. 7. The in vivo post-contrast 3D FLASH MR images of the KEG5 and Dotarem over time.

KEG5 showed excellent contrast of the vascular lumen with main aortic branches and persistent vascular enhancement from the immediate post-contrast phase to the 90 minute delayed phase. Dotarem showed vascular enhancement just on the immediate post-contrast phase and nearly washed out from the vascular structures on 5 minute images.

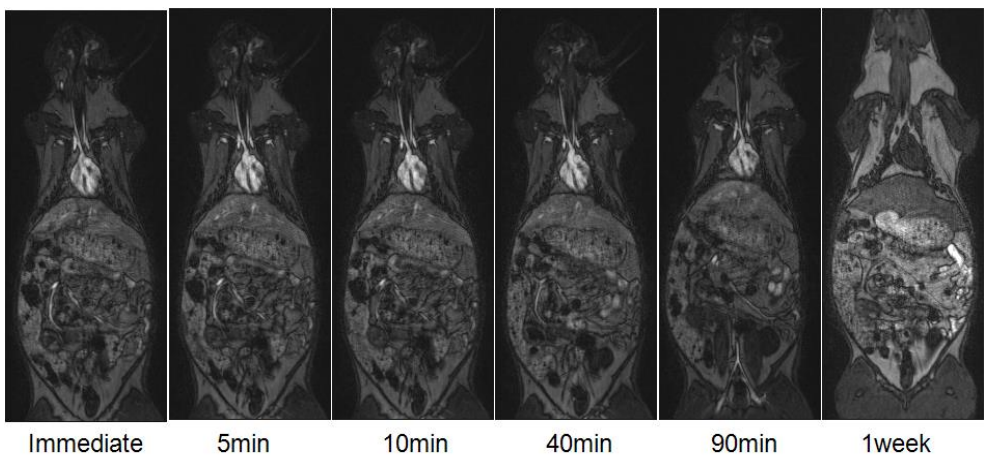

KEG5

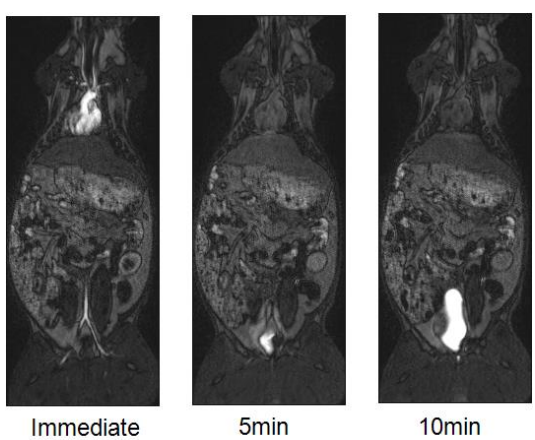

Dotarem

Fig. 8. Comparison of the vascular enhancement over time between KEG5 and Dotarem.

KEG5 showed persistent high signal intensities after peak signal intensity until 90 minute image, but Dotarem showed abruptly decreased signal intensities after peak signal intensity.

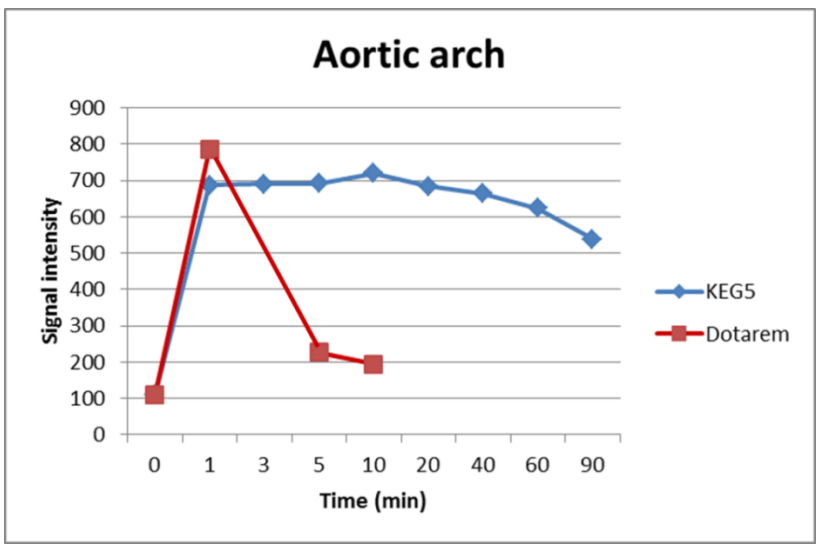

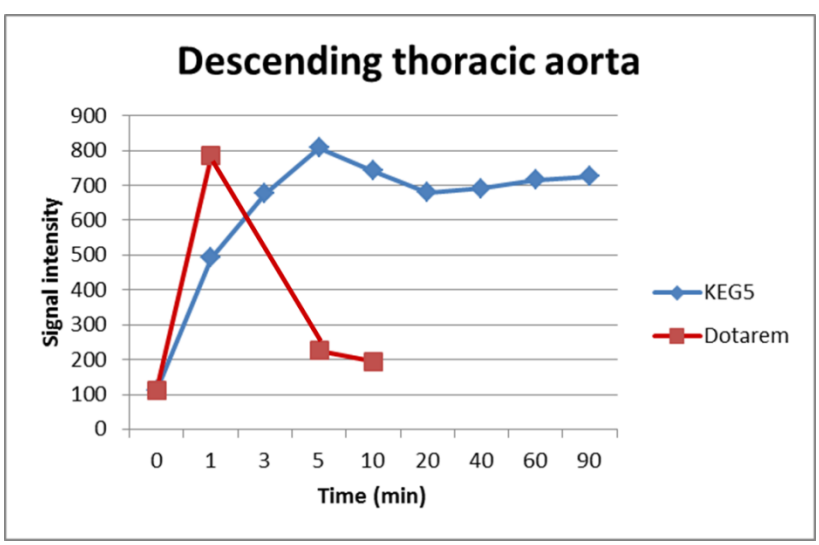

Fig. 9. Comparison of the organ and vascular enhancement between KEG5 and Dotarem on the immediate post-contrast images.

KEG5 showed similar enhancement compare to Dotarem at all measured regions in immediate post-contrast images.

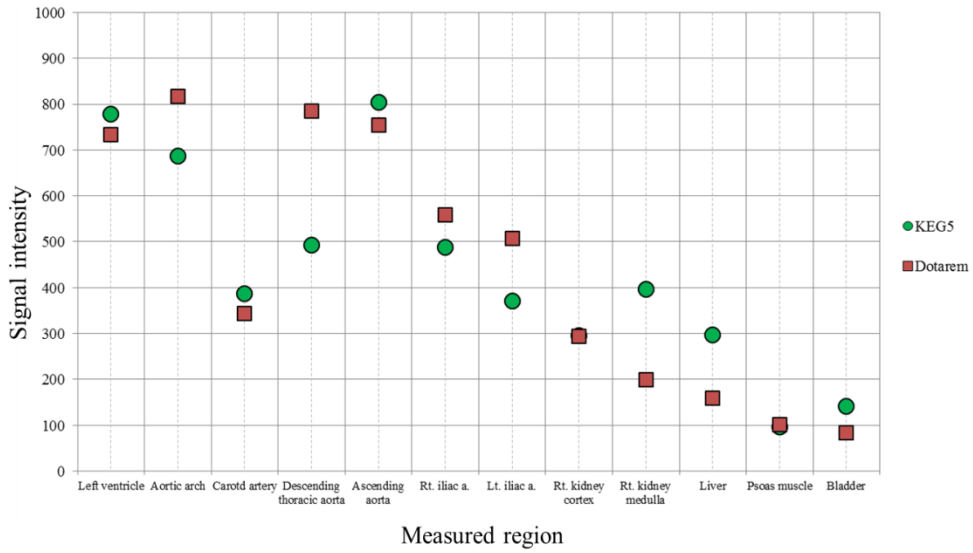

Fig. 10. The MR images obtained from in vivo cross-over experiment.

On the immediate post-contrast images, KEG1-S, KEG3-S, and DOT-S showed peak signal intensity. On the statistical analysis, there was no significant difference of signal intensities between KEG3-S and DOT-S ($p=1.000$), but KEG1-S showed significantly lower peak signal intensity than KEG3-S and DOT-S ($p<0.05$). KEG1-S and KEG3-S showed persistent delayed enhancement, whereas DOT-S showed rapid washout after immediate post-contrast images.

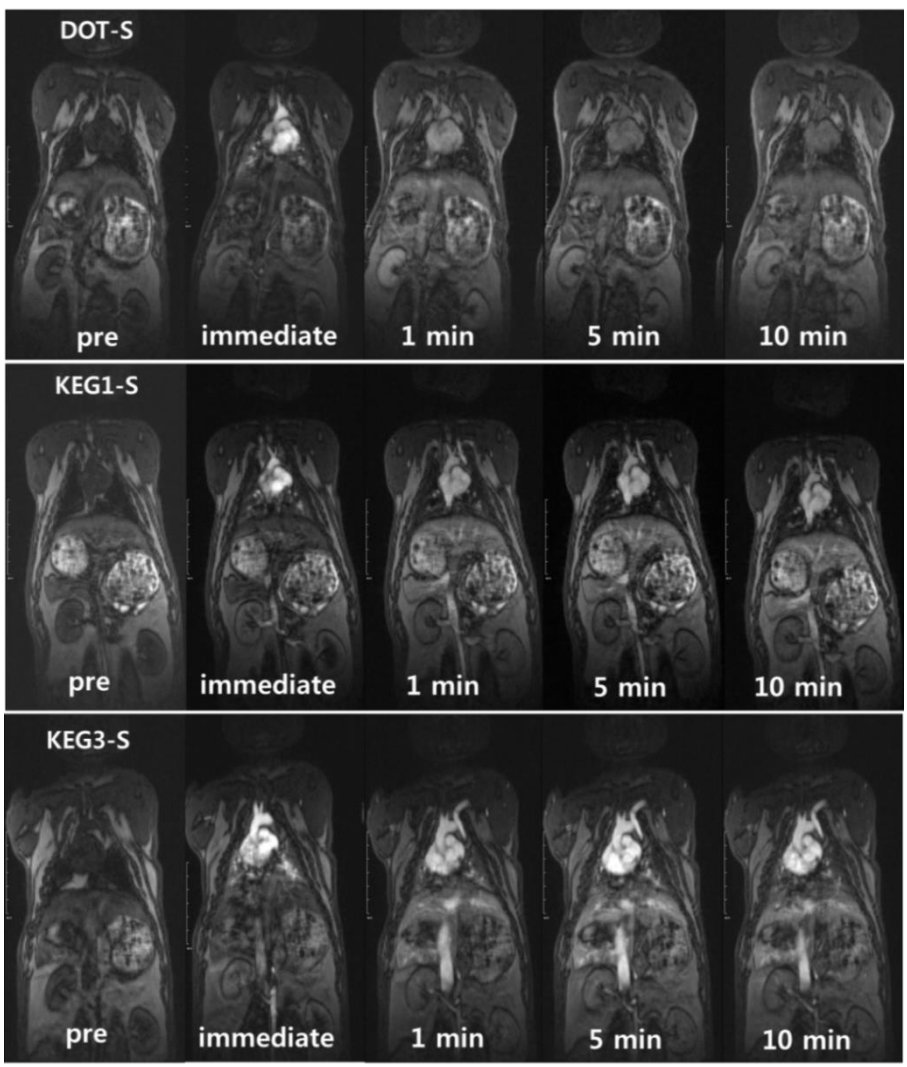

DOT-S – 0.1 mmol/kg Gd-DOTA, KEG1-S – 0.093 mmol/kg KEG1, KEG3-S – 0.093 mmol/kg KEG3

Fig. 11. Signal intensity changes at aortic arch and descending thoracic aorta in cross-over animal experiment.

All ESIONs showed slightly decreased signal intensities and maintained plateau after peak signal intensity until post-contrast 10 minute images, whereas Dotarem showed abruptly decreased signal intensities after peak signal intensity. On the statistical analysis, all half-diluted contrast material showed significantly lower signal intensities than their non-diluted ones on immediate and delayed phase images ($p<0.05$). KEG3-S showed similar peak signal intensity compare to DOT-S on first-pass imaging ($p=1.000$) and higher signal intensity on delayed imaging ($p<0.001$).

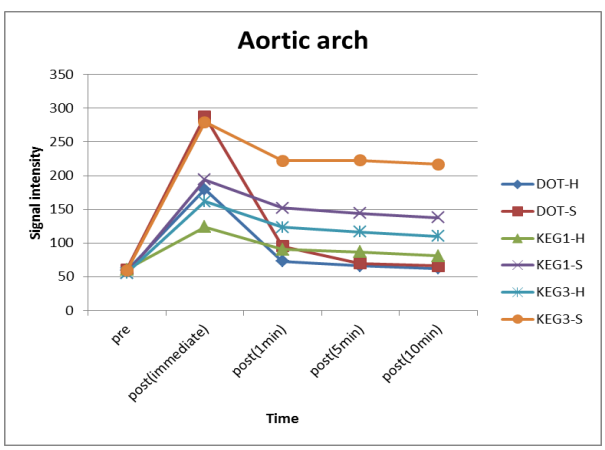

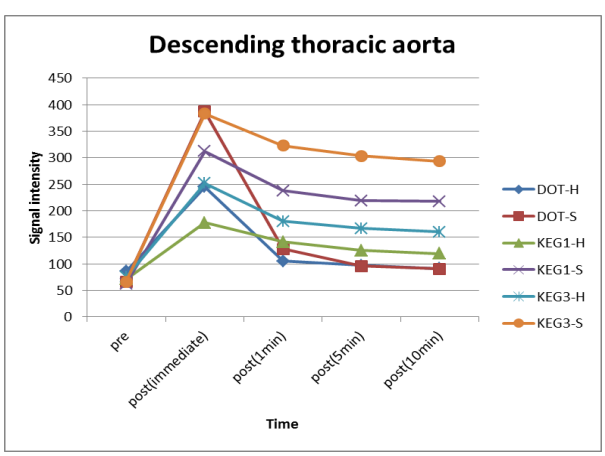

DOT-H – 0.05 mmol/kg Gd-DOTA, DOT-S – 0.1 mmol/kg Gd-DOTA, KEG1-H – 0.047 mmol/kg KEG1, KEG1-S – 0.093 mmol/kg KEG1, KEG3-H – 0.047 mmol/kg KEG3, KEG3-S – 0.093 mmol/kg KEG3

Discussion

CE-MRA is well established safe and effective tool for the diagnosis of the various vascular diseases because it does not use radiation and shows better images for the calcified segment compared with the CT angiography (15-18). Typically, it is performed using GBCA to maximize the contrast of the vascular structure from the surrounding soft tissue through the T1 shortening effect. However, GBCAs have several limitations including short temporal window for data acquisition and potential toxicity causing NSF in patients with ESRD due to the free gadolinium ion. For these reasons, the needs for the new alternative MR contrast material have been emerged.

The MR contrast agents are generally categorized according to their effects on longitudinal (T1) and transversal (T2) relaxations, and their ability is referred to as relaxivity (r_1, r_2). In the MR images, fast T1 relaxation cause bright signal intensity and fast T2 relaxation cause dark signal intensity. It is reported that the parameter r_2/r_1 gives indication as to whether the contrast agents become positive or negative agents. According to the previous study, brightening is observed in the T1-weighted images when the r_2/r_1 value below about two (19). Therefore, for becoming the ideal T1 contrast agent, high longitudinal relaxivity (r_1) or low r_2/r_1 value is needed.

The common iron oxide nanoparticles are not appropriate for the T1 MR contrast agents because the high r_2 of iron nanoparticles derived from innate high magnetic moment prevents them from being utilized as T1 contrast agents. However, in the

nanoscale regime, surface spin-canting effects of nanoparticles have a significant effect on their magnetic moment and MR contrast enhancement (20). As the size of nanoparticle decreases, the surface effect becomes more pronounced and is reflected in the reduced net magnetic moment. Therefore, the small size iron oxide nanoparticles can enhance the T1 effect by their large surface area and suppress the T2 effect by their small magnetic moment. For these reasons, small size iron oxide nanoparticles are the potential candidate for T1 contrast agents.

In our study, we used ESIONs with 3 – 4 nm iron oxide core and, theoretically, these were expected to have T1 shortening effect owing to its nanoscale size which cause the reduced net magnetic moment. Our experiment showed the ESIONs had good physical characteristics as a T1 contrast agent with high r_1 value and low r_2/r_1 ratio. Our experimental ESIONs were synthesized by controlled thermal decomposition of iron-oleate complex, and this synthetic technique could be lead to the uniformity in the size of the ESIONs, which is critical for the fine control of the MR relaxivity (21).

In the phantom study, the relaxivity ratios (r_2/r_1) of the ESIONs increased with increasing magnetic field strengths owing to decreasing relaxivity $r1$ values. Theoretically, it may be expected that T1 contrast effect of ESONs is lower at 4.7T than at 1.5T. According to the previous studies for the effect of magnetic field strength on the relaxivity, decreasing relaxivity r_1 value with increasing magnetic field strength is common in GBCA (22), and our experiments with ESIONs and Dotarem® showed same results with previous studies. However, MR signal

depends on several MR-related factors and concentration of contrast material, the further studies should be performed in the clinical setting.

The most common technique of CE-MRA is gradient echo imaging because of rapid image acquisition. In the GRE sequence, the optimal flip angle is determined with reference to the Ernst angle equation to maximized contrast enhancement and usually ranged between 15° and 25°. In our in vitro MR imaging with GRE sequence, MR imaging was performed with wide range dilutions of ESIONs in variable flip angles. The results showed that the peak signal intensities were observed in higher flip angles with an increase of concentration of ESIONs at both of 1.5T and 3T, and this was similar to the Dotarem®. With this result, it could be predicted that the ESIONs have similar contrast enhancement effect in the current clinical protocol for CE-MRA. However, in case of clinical application, other MR parameters should be considered for the determination of the optimal flip angle.

In the in vivo kinetics study and the cross-over experiment, the ESIONs showed compatible vascular enhancement compared to GBCA on the first-pass MRA and the similar organ enhancement pattern after immediate post-contrast images on the objective and subjective evaluation. With this results, the clinical application of ESIONs as a blood pool contrast agent is regarded as reasonable and feasible. In addition, ESIONs showed persistent intravascular enhancement more than 90 minutes, which made it possible to perform delayed imaging for the vascular structures. Originally, ESIONs are hydrophobic and the PEG ligand was introduced via the ligand exchange reaction to make the ESIONs dispersible in aqueous media

for various biomedical applications (23). With this, the half-life of ESIONs in the blood could also be increased by avoiding uptake by the reticuloendothelial (RES) system (24) and, as a result, ESIONs could be used for repeated imaging and high resolution imaging that needs long scan time.

With the property of persistent delayed enhancement, the clinical indications of ESIONs might be different from GBCA. For example, in terms of the use of ESIONs in acute myocardial infarction (AMI), there are some limitations unlike GBCA. In the cardiac MRI used GBCA, the healthy myocardium shows rapid washout of GBCA whereas areas of infarcted myocardium exhibit delayed enhancement 10-15 minutes after the injection (25). As the ESIONs shows persistent enhancement of the blood pool area more than 90 minutes, it might be difficult to differentiate infarcted myocardium from adjacent ventricular chamber in delayed phase. However, recent experimental study showed the feasibility for potential use of ESIONs as a blood pool agent in coronary MR angiography with equivalent quality on first pass images and better delayed images compare with GBCA (26). In addition, USPIOs can be used as a T2 negative agent on T2*- and T2-weighted images owing to its T2 shortening effect, and has potential applications in macrophage and lymph node imaging in various pathology (27-30).

Originally, some USPIOs were developed as an intravenous iron-replace therapy for anemic patients with chronic kidney disease (31). For example, ferumoxytol (Feraheme^{TM}) was FDA-approved superparamagnetic iron oxide nanoparticle-based MR contrast agent that is also employed in the treatment of iron deficiency

anemia. In our study, the single dose of ESIONs in MRA for animal was 0.093 mmol/kg (5.2 mgFe/kg) and, if it is administered in adult with 70 kg body weight, total dose would be 364 mg. Compared with commercially used intravenous iron preparation, the single dose of ESIONs is less than the maximum dose of commercially used one per week (i.e. Feroba® 7 mgFe/kg per week). Therefore, our experimental ESIONs can be used not only as a MR contrast agent but also as an intravenous preparation for patients with iron deficiency anemia.

In terms of adverse effects of contrast materials, GBCA can cause NSF because of the toxic free gadolinium ion in patients with renal dysfunction (32). Half-life of GBCA is about 90 minutes in patients with normal renal function, but it is prolonged from 30 to 120 hours in patients with chronic renal failure. During this time, dissociated free gadolinium ion can compete with calcium ion and cause NSF. On the contrary, ESIONs have no risk of NSF despite of its long half-life in the blood. According to the recent guidelines based on the several studies, the risk of NSF in the use of macrocyclic GBCAs is quite low even in the patients with acute or chronic kidney disease and macrocyclic GBCA can be administered when GBCA is necessary and there is no alternative test (33-38). However, they also recommend that the informed consent should be obtained for the chance of developing NSF and dialysis should be scheduled within 2-3 hours after GBCA administration in these at-risk patients (39). In addition, some researchers discussed that the incidence of NSF is decreased recently by virtue of regulatory action and practice changes in the use of GBCA (40). From this point of view, there are

possibility of clinical application of ESIONs as an alternative contrast agent in the patients with acute kidney injury or chronic kidney disease with estimated glomerular filtration rate (eGFR) less than 30 ml/min/1.73m^2 or those on dialysis as well as a primary contrast agent in the studies that need long scan time or high resolution images.

Despite of some advantages of ESIONs over GBCA, there have been safety concerns about the potential toxicity of the iron oxide nanoparticles (41, 42). The most intracellular and in vivo nanotoxicities from iron oxide nanoparticles are caused by oxidative stress from the excessive production of reactive oxygen species (ROS) (43). However, ferritin and transferrin receptors regulate the homeostasis of iron and, eventually, the iron is incorporated in hemoglobin. According to a study, cytotoxic effect was not observed when Fe_3O_4 and $MnFe_2O_4$ nanoparticles are tested up to the concentration of 200 μgmL^{-1} (20, 44). In addition, as the interactions between nanoparticles and biological organisms take place at the surface of iron oxide nanoparticles, proper surface coating can stabilize iron oxide nanoparticles and toxic reaction. For example of coating material, PEG is Food and Drug Administration (FDA) approved surface coating polymer that generally does not induce any toxicity. ESIONs used in our study have PEG ligand as a surface coating polymer and there was no acute adverse reaction and ESIONs related death of the experimental animals. Another concern is accumulation of iron in the liver and this can cause alteration of the signal intensity of contrast MR images after administration. According to the previous study, although there was no adverse

reaction to iron based MR contrast agents, MR relaxation rates were influenced from 3 to 11 month compared with baseline values (42). But, in our animal study, there was no significant signal alteration in the liver on one week follow up images. However, for the clinical application of the ESIONs in human, further studies for the safety issues and long term effects are required.

In conclusion, on the phantom study, the ESIONs with 3 – 4 nm iron oxide cores showed good T1 shortening effect with the relaxivity ratios (r_2/r_1) 6 or less than 6 at 1.5T and 3T. On in vivo experiment, the ESION with 3 nm iron core and 10 nm overall size (KEG3) showed comparable performance on the first-pass imaging and superior performance on delayed imaging to the commercially available T1 MR contrast agent (Dotarem®) at 3T.

References

1. Gozzi M, Amorico MG, Colopi S, Favali M, Gallo E, Torricelli P, Polverini I, Gargiulo M. Peripheral arterial occlusive disease: role of MR angiography. Radiol Med. 2006;111(2):225-37.

2. Lim RP, Shapiro M, Wang EY, Law M, Babb JS, Rueff LE, Jacob JS, Kim S, Carson RH, Mulholland TP, Laub G, Hecht EM. 3D time-resolved MR angiography (MRA) of the carotid arteries with time-resolved imaging with stochastic trajectories: comparison with 3D contrast-enhanced Bolus-Chase MRA and 3D time-of-flight MRA. AJNR Am J Neuroradiol. 2008;29(10):1847-54.

3. Nael K, Fenchel M, Krishnam M, Finn JP, Laub G, Ruehm SG. 3.0 Tesla high spatial resolution contrast-enhanced magnetic resonance angiography (CE-MRA) of the pulmonary circulation: initial experience with a 32-channel phased array coil using a high relaxivity contrast agent. Invest Radiol. 2007;42(6):392-8.

4. Prince MR. Gadolinium-enhanced MR aortography. Radiology. 1994;191(1):155-64.

5. Yucel EK. MR angiography for evaluation of abdominal aortic aneurysm: has the time come? Radiology. 1994;192(2):321-3.

6. Government of Canada. Gadolinium-Containing Contrast Agents—Update on Nephrogenic Systemic Fibrosis/Nephrogenic Fibrosing Dermopathy

(NSF/NFD)—Notice to Hospitals. http://healthycanadians.gc.ca/recall-alert-rappel-avis/hcsc/2013/36711a-eng.php. Published 2013.

7. U.S. Department of Health and Human Services. FDA Drug Safety Communication: New Warnings for Using Gadolinium-Based Contrast Agents in Patients With Kidney Dysfunction. https://www.fda.gov/Drugs/DrugSafety/ucm223966.htm. Published 2010.
8. European Medicines Agency. Gadolinium-Containing Contrast Agents. http://www.ema.europa.eu/ema/index.jsp?curl=pages/medicines/human/referrals/Gadolinium-containing contrast agents/human_referral_000182.jsp. Published 2010.
9. Khawaja AZ, Cassidy DB, Al Shakarchi J, McGrogan DG, Inston NG, Jones RG. Revisiting the risks of MRI with Gadolinium based contrast agents-review of literature and guidelines. Insights Imaging. 2015;6(5):553-8.
10. Wang Y, Alkasab TK, Narin O, et al. Incidence of nephrogenic systemic fibrosis after adoption of restrictive gadolinium-based contrast agent guidelines. Radiology. 2011;260(1):105-11.
11. Altun E, Martin DR, Wertman R, Lugo-Somolinos A, FullerER III, Semelka RC. Nephrogenic systemic fibrosis: change in incidence following a switch in gadolinium agents and adoption of a gadolinium policy—report from two U.S. universities. Radiology. 2009;253(3):689-96.
12. Roch A, Muller RN. Theory of proton relaxation induced by superparamagnetic particles. J Chem Phys. 1999; 110:5403

13. Antell H, Numminen J, Abo-Ramadan U, Niemelä MR, Hernesniemi JA, Kangasniemi M. Optimization of high-resolution USPIO magnetic resonance imaging at 4.7 T using novel phantom with minimal structural interference. J Magn Reson Imaging. 2010;32(5):1184-96.
14. Ling D, Park W, Park YI, Lee N, Li F, Song C, Yang SG, Choi SH, Na K, Hyeon T. Multiple-interaction ligands inspired by mussel adhesive protein: synthesis of highly stable and biocompatible nanoparticles. Angew Chem Int Ed Engl. 2011;50(48):11360-5.
15. Bremerich J, Bilecen D, Reimer P. MR angiography with blood pool contrast agents. Eur Radiol. 2007;17(12):3017-24.
16. Kim WY, Danias PG, Stuber M, Flamm SD, Plein S, Nagel E, Langerak SE, Weber OM, Pedersen EM, Schmidt M, Botnar RM, Manning WJ. Coronary magnetic resonance angiography for the detection of coronary stenoses. N Engl J Med. 2001;345(26):1863-9.
17. Liu X, Zhao X, Huang J, Francois CJ, Tuite D, Bi X, Li D, Carr JC. Comparison of 3D free-breathing coronary MR angiography and 64-MDCT angiography for detection of coronary stenosis in patients with high calcium scores. AJR Am J Roentgenol. 2007;189(6):1326-32.
18. Sakuma H, Ichikawa Y, Chino S, Hirano T, Makino K, Takeda K. Detection of coronary artery stenosis with whole-heart coronary magnetic resonance angiography. J Am Coll Cardiol. 2006;48(10):1946-50.
19. Hifumi H, Yamaoka s, Tanimoto A, Citterio D, Suzuki K. Gadolinium-based

hybrid nanoparticles as a positive MR contrast agent. J Am Chem Soc. 2006;128(47):15090-1.

20. Jun YW, Lee JH, Cheon JW. Chemical design of nanoparticle probes for high-performance magnetic resonance imaging. Angew Chem Int Ed Engl. 2008; 47:5122-35.
21. Kim BH, Lee NH, Kim HS, An KJ, Park YI, Choi YS, Shin KS, Lee YJ, Kwon SG, Na HB, Park JG, Ahn TY, Kim YW, Moon WK, Choi SH, Hyeon TH. Large-scale synthesis of uniform and extremely small-sized iron oxide nanoparticles for high-resolution T1 magnetic resonance imaging contrast agents. J Am Chem Soc. 2011;133:12624-31.
22. Hagberg GE, Scheffler K. Effect of r1 and r2 relaxivity of gadolinium-based contrast agents on the T1-weighted MR signal at increasing magnetic field strengths. Contrast Media Mol Imaging. 2013;8(6):456-65.
23. Na HB, Lee IS, Seo H, Park YI, Lee JH, Kim SW, Hyeon T. Versatile PEG-derivatized phosphine oxide ligands for water-dispersible metal oxide nanocrystals. Chem Commun (Camb). 2007;48:5167-9.
24. Pouliquen D, Le Jeune JJ, Perdrisot R, Ermias A, Jallet P. Iron oxide nanoparticles for use as an MRI contrast agent: pharmacokinetics and metabolism. Magn Reson Imaging. 1991;9(3):275-83.
25. Mahrholdt H, Wagner A, Holly TA, Elliott MD, Bonow RO, Kim RJ, Judd RM. Reproducibility of chronic infarct size measurement by contrast-enhanced magnetic resonance imaging. Circulation. 2002;106(18):2322-7.

26. Park EA, Lee W, So YH, Lee YS, Jeon BS, Choi KS, Kim EG, Myeong WJ. Extremely Small Pseudoparamagnetic Iron Oxide Nanoparticle as a Novel Blood Pool T1 Magnetic Resonance Contrast Agent for 3 T Whole-Heart Coronary Angiography in Canines: Comparison With Gadoterate Meglumine. Invest Radiol. 2017 Feb;52(2):128-133.

27. Yoo RE, Cho HR, Choi SH, Won JK, Kim JH, Sohn CH. Optimization of ultrasmall superparamagnetic iron oxide (P904)-enhanced magnetic resonance imaging of lymph nodes: initial experience in a mouse model. Anticancer Res. 2014;34(10):5389-96.

28. Khurana A, Nejadnik H, Gawande R, et al. Intravenous ferumoxytol allows noninvasive MR imaging monitoring of macrophage migration into stem cell transplants. Radiology. 2012;264:803-11.

29. Richards JM, Shaw CA, Lang NN, et al. In vivo mononuclear cell tracking using superparamagnetic particles of iron oxide: feasibility and safety in humans. Circ Cardiovasc Imaging. 2012;5:509-17.

30. Sosnovik DE, Nahrendorf M. Cells and iron oxide nanoparticles on the move: magnetic resonance imaging of monocyte homing and myocardial inflammation in patients with ST-elevation myocardial infarction. Circ Cardiovasc Imaging. 2012;5:551-4.

31. Neuwelt EA, Hamilton BE, Varallyay CG, et al. Ultrasmall superparamagnetic iron oxides (USPIOs): a future alternative magnetic resonance (MR) contrast agent for patients at risk for nephrogenic systemic fibrosis (NSF)? Kidney Int.

2009;75:465-74.

32. Malikova H, Holesta M. Gadolinium contrast agents - are they really safe? J Vasc Access. 2017;18(Suppl. 2):1-7.

33. Schieda N, Blaichman JI, Costa AF, Glikstein R, Hurrell C, James M, Jabehdar Maralani P, Shabana W, Tang A, Tsampalieros A, van der Pol C, Hiremath S. Gadolinium-Based Contrast Agents in Kidney Disease: Comprehensive Review and Clinical Practice Guideline Issued by the Canadian Association of Radiologists. Can Assoc Radiol J. 2018;69(2):136-50.

34. Nandwana SB, Moreno CC, Osipow MT, Sekhar A, Cox KL. Gadobenate Dimeglumine Administration and Nephrogenic Systemic Fibrosis: Is There a Real Risk in Patients with Impaired Renal Function? Radiology. 2015;276(3):741-7.

35. Janus N, Launay-Vacher V, Karie S, Clement O, Ledneva E, Frances C, Choukroun G, Deray G. Prevalence of nephrogenic systemic fibrosis in renal insufficiency patients: results of the FINEST study. Eur J Radiol. 2010;73(2):357-9.

36. Deray G, Rouviere O, Bacigalupo L, Maes B, Hannedouche T, Vrtovsnik F, Rigothier C, Billiouw JM, Campioni P, Ferreiros J, Devos D, Alison D, Glowacki F, Boffa JJ, Marti-Bonmati L. Safety of meglumine gadoterate (Gd-DOTA)-enhanced MRI compared to unenhanced MRI in patients with chronic kidney disease (RESCUE study). Eur Radiol. 2013;23(5):1250-9.

37. Amet S, Launay-Vacher V, Clément O, Frances C, Tricotel A, Stengel B, Gauvrit JY, Grenier N, Reinhardt G, Janus N, Choukroun G, Laville M, Deray G. Incidence of nephrogenic systemic fibrosis in patients undergoing dialysis after contrast-enhanced magnetic resonance imaging with gadolinium-based contrast agents: the Prospective Fibrose Nephrogénique Systémique study. Invest Radiol. 2014;49(2):109-15.
38. Soyer P, Dohan A, Patkar D, Gottschalk A. Observational study on the safety profile of gadoterate meglumine in 35,499 patients: The SECURE study. J Magn Reson Imaging. 2017;45(4):988-97.
39. Schieda N, Maralani PJ, Hurrell C, Tsampalieros AK, Hiremath S. Updated Clinical Practice Guideline on Use of Gadolinium-Based Contrast Agents in Kidney Disease Issued by the Canadian Association of Radiologists. Can Assoc Radiol J. 2019;70(3):226-32.
40. Attari H, Cao Y, Elmholdt TR, Zhao Y, Prince MR. A Systematic Review of 639 Patients with Biopsy-confirmed Nephrogenic Systemic Fibrosis. Radiology. 2019;292(2):376-86.
41. Liu G, Gao J, Ai H, Chen X. Applications and potential toxicity of magnetic iron oxide nanoparticles. Small. 2013;9(9-10):1533-45.
42. Storey P, Lim RP, Chandarana H, Rosenkrantz AB, Kim D, Stoffel DR, Lee VS. MRI assessment of hepatic iron clearance rates after USPIO administration in healthy adults. Invest Radiol. 2012;47(12):717-24.
43. Sharifi S, Behzadi S, Laurent S, Forrest ML, Stroeve P, Mahmoudi M. Toxicity

of nanomaterials. Chem Soc Rev. 2012;41(6):2323-43.

44. Lee JH, Huh YM, Jun YW, Seo JW, Jang JT, Song HT, Kim S, Cho EJ, Yoon HG, Suh JS, Cheon J. Artificially engineered magnetic nanoparticles for ultra-sensitive molecular imaging. Nat Med. 2007;13(1):95-9.

국문초록

연구배경 및 목적: 자기공명영상조영제는 자기장에 미치는 영향에 따라 상자성, 초상자성 제제로 구분이 되며, 현재 가장 널리 사용되는 조영제는 가돌리니움을 이용한 상자성 조영제이다. 가돌리니움은 유리이온의 형태에서 독성이 매우 높아서 가돌리니움-킬레이트의 형태로 사용이 되고 있다. 가돌리니움 조영제의 체내반감기는 정상인에서 약 90분이지만 만성신부전 환자에서는 30-120시간까지 연장되어있어, 체내 여러 조직에서 장기간 체류하면서 가돌리니움 유리이온이 배출되어 전신섬유화를 일으킬 수 있다. 이러한 배경에서, 가돌리니움 기반의 자기공명영상조영제는 신원성 전신섬유화의 원인 물질로 간주되어 왔다. 최근 거대고리를 가진 가돌리니움 기반의 자기공명영상조영제를 사용하게 됨에 따라 신원성 전신섬유화의 발생빈도가 상당히 감소하였지만, 고위험 환자에서의 사용 자제 및 과다한 용량의 투여를 제한한 것도 주요한 요인이라고 할 수 있다. 가돌리니움 기반의 자기공명영상조영제와는 달리 초상자성 제제는 다양한 크기의 산화철입자를 이용하는데, 만성신부전 환자에서 경정맥투여에 대한 안전성이 확립되어있으며, 이 중에서도 최근 50 nm이하의 크기를 가지는 제제가 개발되어 혈액저류 자기공명영상조영제로서의 이용에 대한 연구가 진행되고 있다. 본 연구의 목적은 새롭게 합성된 3 – 4 nm 크기의 철분핵을 가진 균일한 미세철분기반 나노입자의

자기공명특성 및 자기공명혈관조영술 조영제로서의 적합성을 모형실험과 동물실험을 통하여 평가하는 데 있다.

방법: 7종의 철분기반 나노입자 (KEG1 – 7)를 이용하여 1.5T, 3T, 및 4.7T 자기공명영상장치에서 모형 및 동물실험을 시행하였다. 각 나노입자당 순차적으로 희석된 시료를 제작한 후, inversion-recovery turbo spin-echo (IR-TSE), multiple echo-spin echo (ME-SE), multislice multiecho (MSME) 시퀀스를 이용하여 자기공명특성을 분석하였다. 경사에코 시퀀스를 이용하여 모형실험에서 낮은 relaxivity ratio (r_2/r_1)를 보인 2종의 선택된 철분기반 나노입자 (KEG1, KEG5)의 다양한 숙임각 및 농도에서의 자기공명신호강도 변화를 평가하였다. 모형실험에서 낮은 relaxivity ratio (r_2/r_1)를 보인 3종의 선택된 철분기반 나노입자 (KEG1, KEG3, KEG5)를 이용하여, 총 8마리의 몸무게 3kg의 가토를 대상으로 체내 약동학적 특성 평가 및 체내교차시험을 시행하였다. 약동학적 특성 평가는 1종의 철분기반 나노입자 (KEG5)를 이용하였고, 가토에 투여한 후, 시간경과에 따른 혈관의 조영정도, 체내 장기의 조영증강 정도, 체외배출 등을 평가하였다. 체내교차시험은 2종의 철분기반 나노입자 (KEG1, KEG3)와 도타렘의 원액 (KEG1-S, KEG3-S – 0.093 mmol/kg; DOT-S – 0.1 mmol/kg) 및 1/2 희석된 시료 (KEG1-H, KEG3-H – 0.047 mmol/kg; DOT-H – 0.05 mmol/kg)를 제작하여 가토에 교차투여

한 후, 시간경과에 따른 혈관의 조영증강 정도를 측정하고, 조영제 간의 차이를 linear-mixed effects model을 이용하여 분석하였다. 모형실험 및 동물실험에서 시판중인 자기공명 영상 조영제와 비교를 위하여 도타렘 (Gd-DOTA)을 대조군으로 사용하였다.

결과: 7종의 철분기반 나노입자들의 relaxivity ratio (r_2/r_1)가 1.5T (KEG1, 2.95; KEG2, 6.00; KEG3, 2.44; KEG4, 2.51; KEG5, 1.85; KEG6, 4.37; KEG7, 3.32)와 3T (KEG1, 3.01; KEG2, 5.72; KEG3, 2.68; KEG4, 3.40; KEG5, 3.17; KEG6, 3.76; KEG7, 4.78)에서 모두 6이하로 측정되어 자기공명혈관조영술에 이용이 가능하였다. Relaxivity ratio는 자기장의 세기가 증가할수록 증가하는 경향을 보였다. 경사에코 시퀀스에서, 철분기반 나노입자의 농도가 가장 낮을 때의 최고 신호강도는 1.5T의 경우에 10°에서 20° 사이의 숙임각, 3T의 경우에 10°에서 15° 사이의 숙임각에서 각각 관찰되었다. 철분기반 나노입자의 농도가 증가함에 따라, 더 큰 숙임각에서 최고 신호강도를 보이는 경향이 있었다. 약동학적 특성 평가시에 KEG5는 초회통과 영상에서 최고 자기공명신호를 보인 후, 90분 지연 영상까지 지속적인 혈관의 조영증강을 보였다. KEG5 투여 후 초회통과 영상에서 체내 장기들은 도타렘과 비슷한 정도의 조영증강을 보였다. 1주일 지연 영상에서 KEG5는 거의 모두 체외로 배출되었다. 체내 교차실험에서 1/2 희석된 철분기반 나노입자는 희석이

되지 않은 철분기반 나노입자와 비교하여 유의하게 낮은 조영증강신호를 보였다 (대동맥궁, KEG1-S 대 KEG1-H – difference 70.167, p<0.001 및 KEG3-S 대 KEG3-H – difference 118.167, p<0.001; 하행흉부대동맥, KEG1-S 대 KEG1-H – difference 134.667, p<0.001 및 KEG3-S 대 KEG3-H – difference 131.333, p<0.001). 초회통과 영상에서 최고 신호강도를 측정하였을 때, KEG3-S와 DOT-S 간의 유의한 차이는 보이지 않았고 (대동맥궁, difference -8.167, p=1.000; 하행흉부대동맥, difference -3.667, p=1.000), KEG3-S와 DOT-S는 KEG1-S 보다 높은 신호강도를 보였다 (대동맥궁 및 하행흉부대동맥, p<0.05). 10분 지연 영상에서 KEG3-S와 KEG1-S 모두 DOT-S보다 유의하게 높은 신호강도를 보였다 (대동맥궁, KEG3-S 대 DOT-S – difference 150.667, p<0.001 및 KEG1-S 대 DOT-S – difference 71.667, p<0.001; 하행흉부대동맥, KEG3-S 대 DOT-S – difference 202.667, p<0.001 및 KEG1-S 대 DOT-S – difference 127.333, p<0.001).

결론: 1.5T와 3T 자기공명영상장치에서 시행한 모형실험에서 새롭게 합성된 3 nm 이하의 철분기반 나노입자는 모두 6이하의 relaxivity ratio (r_2/r_1)를 보여 우수한 T1 단축 효과를 보였다. 3T 자기공명영상장치에서 시행한 동물실험에서 3 nm의 철분핵과 10 nm의 전체 크기를 가진 철분기반 나노입자 (KEG3)는 시판중인 T1 자기공명영상 조영제 (도

타렘)와 비교하여 초회통과 영상에서 유사한 조영증강 효과 및 지연영상에서 더 우수한 조영증강 효과를 보였다.

주요어: 산화철나노입자, 혈액저류조영제, 자기공명혈관조영술, 조영증강

학 번: 2010-30524